Research Square

Preprints are preliminary reports that have not undergone peer review.
They should not be considered conclusive, used to inform clinical practice,
or referenced by the media as validated information.

Comparative Micro-CT and Histology Assessment of Bone and Cartilage Alterations in Rat and Rabbit MIA - Induced Osteoarthritis Models

Nor Shahira Solehah Umran
Universiti Putra Malaysia
Mohd Noor Akmal
Universiti Putra Malaysia
Jalila Abu
Universiti Putra Malaysia
Lau Seng Fong
Universiti Putra Malaysia
Faridah Abas
Universiti Putra Malaysia
Iffah Nadhira Madzuki
Universiti Malaysia Perlis
Sharifah Zakiah Sulaiman
Universiti Putra Malaysia
Roslan Yahya
Agency Nuclear Malaysia
Lai Kok Song
Higher Colleges of Technology
Ahmad Fauzi
University of Brawijaya
Mokrish Ajat
mokrish@upm.edu.my

Universiti Putra Malaysia

Article

Keywords: Osteoarthritis (OA), Subchondral bone, Articular cartilage, Micro-computed tomography (micro-CT), Histology, Animal models, Monosodium iodoacetate (MIA)

Posted Date: June 3rd, 2026

DOI: https://doi.org/10.21203/rs.3.rs-9767146/v1

License: This work is licensed under a Creative Commons Attribution 4.0 International License.
Read Full License

Additional Declarations: No competing interests reported.

Comparative Micro-CT and Histology Assessment of Bone and Cartilage Alterations in Rat and Rabbit MIA - Induced Osteoarthritis Models

Authors:

Nor Shahira Solehah Umran[1], Mohd Noor Akmal[1], Jalila Abu[1], Lau Seng Fong[1,6], Faridah Abas[2], Iffah Nadhira Madzuki[4], Sharifah Zakiah Sulaiman[1], Roslan Yahya[5], Lai Kok Song[7], Ahmad Fauzi[8] and Mokrish Ajat[1,3*]

Affiliations:

[1]Faculty of Veterinary Medicine, Universiti Putra Malaysia, 43400 Serdang, Selangor, Malaysia

[2]Faculty of Food Science and Technology, Universiti Putra Malaysia, 43400 Serdang, Selangor, Malaysia

[3]Natural Medicine and Product Research Laboratory, Institute of Bioscience, Universiti Putra Malaysia, 43400 Serdang, Selangor, Malaysia

[4]Faculty of Engineering Technology, Universiti Malaysia Perlis, 02100 Padang Besar, Perlis, Malaysia

[5]Industrial Technology Division, Agency Nuclear Malaysia, Bangi, Selangor, Malaysia

[6]Department of Veterinary Clinical Sciences, Louisiana State University, Baton Rouge, LA, United States

[7]Division of Health Sciences, Higher Colleges of Technology, Abu Dhabi, 25026, United Arab Emirates

[8]Department of Veterinary Clinical Pathology, Faculty of Veterinary Medicine, University of Brawijaya, Malang, East Java 65141, Indonesia

Corresponding Author:

Mokrish Ajat

Email: mokrish@upm.edu.my

ABSTRACT

Osteoarthritis (OA) is a progressive degenerative joint disorder that significantly impairs quality of life and imposes substantial socioeconomic burdens. Animal models are essential tools for evaluating the efficacy of therapeutic agents and nutraceuticals during preclinical development. This study investigates subchondral bone and articular cartilage alterations in monosodium iodoacetate (MIA)-induced OA using rat and rabbit models. Twelve male Sprague Dawley rats and twelve male New Zealand White rabbits received intra-articular injections of MIA (3 mg for rats, 8 mg for rabbits) into the right knee joint. At week 12, joint tissues were harvested and assessed via macroscopic examination, microcomputed tomography (micro-CT), and histological analysis. The findings revealed OA-related changes were more severe in rats, with significantly increased BV/TV, trabecular spacing and porosity compared to rabbits ($p < 0.05$). In contrast, the rabbit model exhibited slower disease progression and more consistent pathological features resembling human OA. Both models effectively replicate OA features, however, the rabbit model provides superior translational relevance for studying OA progression and therapeutic outcomes due to its joint anatomy and disease progression pattern.

Keywords:
Osteoarthritis (OA), Subchondral bone, Articular cartilage, Micro-computed tomography (micro-CT), Histology, Animal models, Monosodium iodoacetate (MIA)

ABBREVIATIONS

ACL – Anterior cruciate ligament
ANOVA – Analysis of variance
BS/BV – Bone surface-to-volume ratio
BV/TV – Bone volume-to-tissue volume ratio
IACUC – Institutional Animal Care and Use Committee
MIA – Monosodium iodoacetate
Micro-CT – Microcomputed tomography
MMP13 – Matrix metalloproteinase 13
OA – Osteoarthritis
PO – Total porosity
Tb.Sp – Trabecular spacing
Tb.Th – Trabecular thickness

1. INTRODUCTION

Osteoarthritis (OA) is a chronic, degenerative joint disease that predominantly affects weight-bearing joints such as the knees, hips, spine, and hands. It is characterized by pain, stiffness, and reduced mobility, which can significantly impair daily function and quality of life. Among these, the knee joint is particularly susceptible to early degeneration due to its critical role in load-bearing and mechanical stress, contributing to progressive wear and tear of the articular cartilage (Clémence et al., 2016). OA is a progressive condition that, if left untreated, can lead to severe joint dysfunction and disability. Hallmark pathological features of OA include degradation of articular cartilage, inflammation of the synovium, subchondral bone sclerosis, calcified cartilage formation, tidemark advancement, and osteophyte development (Kloppenburg & Berenbaum, 2020; Van Den Bosch, 2021).

Research continues to improve the quality of life for individuals affected by OA. OA treatment options include exercise, weight loss programs, pain relief medication, assistive devices, and surgical procedures (Costa et al., 2017). Non-steroidal anti-inflammatory drugs (NSAIDs) may be used for pain and inflammation management, but their long-term use requires careful consideration of potential side effects. NSAIDs' adverse effects, such as urticaria, angioedema, anaphylaxis, cardiovascular issues, and gastroduodenal lesions, have raised concern among patients (Trelle et al., 2011). Therefore, improving our knowledge of OA is important, with ongoing efforts to identify novel therapeutic targets and refine existing interventions.

Animal models are crucial in advancing our comprehension of OA by providing a controlled environment for studying the disease mechanisms, testing potential therapies, and exploring various aspects of OA pathophysiology (Artuzi et al., 2016). Although horses, dogs, goats, and monkeys have joint architecture and function more similarly to humans, they also present greater ethical considerations and are more expensive than smaller animals. Thus, small animals like mice, rats, guinea pigs, and rabbits are often used in pre-clinical trials due to their convenient manageability and cost-effectiveness (Lelovas, 2014). There are two effective OA induction methods: surgical and chemical. Both methods bear their benefits and risks upon induction. Surgical induction models such as meniscal transection and anterior cruciate ligament (ACL) transection are methods that involve incision or cutting the meniscus or ACL in the joint. However, surgical models can cause destabilisation of the joints leading to post-traumatic OA (Wang et al., 2020). The chemical induction model is a method of intra-articular injection of chemicals in the knee joint, commonly monosodium iodoacetate (MIA) (Takahashi et al., 2017). MIA induces chondrocyte death, cartilage degeneration, osteophyte formation, and joint inflammation, resembling aspects of OA. MIA inhibits glyceraldehyde-3-phosphate dehydrogenase of the Kreb cycle that causes chondrocyte death, leading to loss of proteoglycan and cartilage degradation (Kuyinu et al., 2016). In this study, we decided to induce OA with MIA dosages of 3mg and 8mg/knee joint for rats and rabbits, respectively, because it was reported effective, and the result was similar to human OA (Calado et al., 2015; Vinod et al., 2018).

Micro-computed tomography (micro-CT) and histology play crucial roles in improving our understanding of OA by providing detailed insights into the structural and histological changes occurring in joint tissues. Micro-CT provides high-resolution 2D and 3D images of bone structures, including subchondral bone (Jones et al., 2010). This is crucial for understanding changes in bone density, architecture, and the formation of osteophytes, sclerosis, or cysts associated with OA (Musumeci et al., 2013). Moreover, micro-CT allows for quantitative assessment of various parameters, including bone volume, bone mineral density, and trabecular microarchitecture (Karhula et al.,2018). This quantitative data is valuable for studying the progression of subchondral bone changes in OA. Histology provides a detailed examination of joint tissues at both the cellular and tissue levels (Sun et al., 2012). This includes assessing the integrity of articular cartilage, the synovium, ligaments, and other structures within the joint affected by OA (Sulaiman et al., 2021; Sulaiman et al., 2024). Histology staining techniques, such as safranin O, allow for the identification of specific changes in articular cartilage, including loss of proteoglycans, fibrillation, and the exposure of subchondral bone (Rutgers et al.,2010).

Despite decades of research, most OA studies merely focused on the changes in the articular cartilage. However, there is still limited information regarding evaluating changes in articular cartilage and subchondral bone for different animal models. Therefore, this study aims to investigate the subchondral bone and articular cartilage changes in MIA-induced OA rat and rabbit models through macroscopic observation, micro-CT, and histology analysis. This generates an opportunity to learn from these models to extend our understanding of OA pathophysiology and aid in developing targeted therapeutic strategies.

2 MATERIALS AND METHODS

2.1 ANIMALS STUDY DESIGN

The experimental protocol was approved by the Institutional Animal Care and Use Committee (IACUC) of Universiti Putra Malaysia (UPM/IACUC/AUP-R035/2021). A total of 12 male Sprague Dawley rats and 12 male New Zealand White rabbits. All animals were sourced from A-Sapphire Enterprise, Malaysia. All experimental procedures and methods were performed in accordance with relevant institutional guidelines and regulations approved by IACUC.

The rats, weighing between 200–220 g, were housed in groups of three per cage under controlled conditions (27°C, 12-hour light/dark cycle) with exposure to natural sunlight. They were fed standard rat pellets (Gold Coin, Malaysia) and provided with water ad libitum. The rabbits, aged 8–9 months and weighing 1.8–2.0 kg, were individually housed in stainless-steel cages and fed commercial rabbit pellets (Penternakan Hong Lee Sdn. Bhd., Malaysia). Water was also provided ad libitum. All animals were housed at the Animal Research Facility, Faculty of Veterinary Medicine, Universiti Putra Malaysia, and acclimatized for one week before OA induction. Each species was randomly divided into two groups: a control group (n = 6) and an OA-induced group (n = 6), ensuring a randomized and controlled experimental design. The sample size was determined based on previous studies with similar designs,

which demonstrated sufficient statistical power to detect significant OA-related changes. OA was induced via intra-articular injection of MIA into the right knee joint—3 mg for rats and 8 mg for rabbits. These dosages have been validated in prior studies to reliably induce OA-like pathology, including chondrocyte death and cartilage degeneration, mimicking human OA conditions (Dalevich & Dyachenko, 2024; Sulaiman et al., 2022). At 12 weeks post-induction, macroscopic evaluation of joint morphology was performed. Subchondral bone architecture was assessed using micro-CT, while articular cartilage was evaluated histologically to determine the extent of OA-related changes.

2.2 PREPARATION OF OA ANIMAL MODELS

To induce OA, the rats were first anesthetized with Zoletil 50mg/ml (Virbac, Australia) at a dosage of 3 mg/kg of body weight through the intramuscular (i.m.) route. The right knee of each rat was shaved using an electric clipper and sterilized with 75% ethanol. The procedure was then followed by injecting a single dose of 3 mg of MIA (Sigma-Aldrich, Saint Louis, United States) that was dissolved in 50 µl of 0.9% normal saline into the right knee joint using a 26-G needle (Wan Osman et al., 2017). On the other hand, the left knees were not induced for the sake of animal welfare. After inducing OA, the rats were allowed to recover from the anaesthesia in their home cage. Healthy rats were used as a sham control and received 50 µl of 0.9% normal saline in the intra-articular space of the right stifle joint.

The rabbit model also used MIA (Sigma-Aldrich, USA) to induce OA. MIA was dissolved in normal saline to have a concentration of 25 mg/ml. The rabbits were then given an injection of 8 mg per joint per rabbit with a volume of 0.32 ml into the intra-articular space of the right stifle joint. The rabbits were under general anaesthesia using Zoletil (Virbac, Australia) at a dosage of 2 mg/kg intramuscularly during the procedure (Sulaiman et al., 2021). Healthy rabbits were also used as a sham control and were given an injection of 0.32 ml of 0.9% normal saline into the intra-articular space of the stifle joint. The process was carefully conducted to ensure accuracy and consistency, and the rabbits were closely examined during and after the procedure.

2.3 SAMPLE COLLECTION

The animals were carefully examined for any clinical signs of discomfort, such as weight loss or immobility. After 12 weeks, all rats were euthanized through an intraperitoneal injection of 100 mg/kg ketamine and 20 mg/kg xylazine, after which they were humanely sacrificed through intracardiac puncture using 23 G needles. The femur and tibia bones were then carefully dissected to remove all the surrounding soft tissues. The tibia, and femur bone samples were stored at a temperature of -80ºC to ensure their preservation for future analyses.

The rabbits from each group were euthanized using pentobarbital sodium 200 mg/ml (Vetoquinol, France) at a dosage of 120 mg/kg intravenously. The knee joints were then harvested and immediately fixed in 10% buffered formalin (Sigma-Aldrich, USA). After a period of 24 hours, the muscle and tissue surrounding the femur and tibia were carefully removed to avoid any damage to the cartilage surface. The distal femur and proximal tibia were then placed in 10% buffered formalin for further analysis.

2.4 GENERAL CONDITION ASSESSMENT

Throughout the 12-week study period, all animals were monitored daily for morbidity and mortality, recording any signs of abnormal behavior and illness. Weekly physical examinations assessed clinical signs of pain, changes in posture, movement, vocalization, and significant weight loss. Body weights were measured weekly to monitor for any reductions. Joints were carefully examined for effusion, swelling, and warmth, indicative of inflammation.

2.5 MACROSCOPIC OBSERVATION

At week 12, the femoral and tibial plateau were thoroughly analysed using a Quad camera with 108 megapixels to detect any gross pathologic changes. The articular cartilage was observed to identify any signs of erosion and osteophyte formation. The evaluation was based on the Modified Outerbridge score introduced by Uhl et al. in 2004 (Table 1).

Table 1: Modified Outerbridge scale for assessing cartilage damage severity.

Score	Indication
0	Normal cartilage with a smooth surface
1	Slight softening and swelling but no fibrillation or damage to the cartilage surface
2	Partial-thickness defects with fissures on the surface not reaching subchondral bone or >1.5 cm
3	More severe cartilage damage with fissures down to subchondral bone, defects <50% cartilage depth
4	Complete loss of cartilage with exposure of subchondral bone

2.6 MICRO-CT EVALUATION

The frozen bone samples of the right femur and tibia were defrosted on ice, soaked in saline solution, and then wiped down with multi-fold paper towels to remove any debris from the surface of the bones. The bones were then wrapped in parafilm to keep them hydrated during the scanning process.

For the rat model, the bone was scanned using a SkyScan 1076 micro-CT scanner (SkyScan, Kontich, Belgium) with a voltage of 72 kV and 130 µA current tube. The pixel size used was 18 µm, and a rotation step of 0.5° was used for a full 360° rotation. The scanning process produced 2D and 3D images that were evaluated qualitatively using Data-Viewer and CTVox software (Skyscan, Belgium) in axial, coronal, and sagittal views.

For the rabbit model, each femur and the proximal part of each tibia of the stifle joint was scanned with a pixel size of 14.7 µm. The current used was 118 µA with a 0.5 mm aluminium filter, and the X-ray tube voltage was 85 kV. The exposure time was 500 ms, and X-ray projections were obtained at intervals of 0.7 degrees over a scanning angular range of 360 degrees. The resulting data were then reconstructed with Skyscan NRecon software (Skyscan, Belgium).

The reconstructed dataset was evaluated qualitatively using Data-Viewer and CTVox software in axial, coronal, and sagittal views to identify and describe the joint lining and the presence or absence of osteophytes in different experimental groups. Two-dimensional (2D and 3D) images were used for morphological changes.

Micro-CT images were also analysed quantitatively using Skyscan CT-Analyser Software (Skyscan, Luxembourg, Belgium). To do this, a stack of regions of interest (ROI) within a volume of interest (VOI) was selected from the distal femoral subchondral bone at the epiphyseal using a semi-automatic contouring method. The parameters of subchondral bone micro-architecture that were analysed included the ratio of bone volume over tissue volume (BV/TV; %), the bone surface-to-volume ratio (BS/BV; mm2/ mm3), trabecular thickness (Tb. Th; mm), trabecular spacing (Tb. Sp; mm), and total porosity (PO; %).

2.7 HISTOLOGICAL ASSESSMENT OF THE CARTILAGE

The femur and tibia from the harvested joint were immediately fixed in 10% buffered formalin (Sigma-Aldrich, USA) to prevent degradation of the tissue. The fixation process was carried out for two weeks to ensure complete fixation. After the fixation process, the bones were decalcified with 10% formic acid

(Nacalai Tesque, Japan). The decalcification process lasted ten days, and the 10% formic acid was changed every two days.

Before embedding, the surrounding tissue around the joint was meticulously removed to ensure that the bones were clean and free from any debris. Once the bones were clean, the tibia and femur were separated in a dorsal plane. The bones were then placed in labelled cassettes for easy tracking. These cassettes were soaked in 80% alcohol and 95% alcohol for two hours each, followed by 100% alcohol for three hours, chloroform solution for three hours, and paraffin solution for five hours and 30 minutes. This process ensured that the bones were completely dehydrated and that the solution could infiltrate the bones.

Afterwards, the bones were embedded in paraffin using Leica EG1150H and EG11559 Modular Tissue Embedding Center (Leica Biosystems, Germany). Sections of 5 µm thickness were made using a microtome (Leica Jung Multicut 2045, Germany). These sections were then stained with Hematoxylin & Eosin (H&E) and safranin O (safranin O staining kit, ScienCell Research Laboratories, California). The slides were dehydrated and cleared with 95% ethyl alcohol and absolute ethyl alcohol, alternately at 2 minutes each for two times. Finally, the slides were mounted using a mixture of Distyrene, a plasticizer, and xylene (DPX) as the mounting medium. The histomorphometric parameters were observed under a light microscope with an image analyser (Motic, China) under 200x magnification. Histological grade (modified from Pritzker et al., 2006) were used to assess the histological alterations in the articular cartilage rat and rabbit animal models (n = 6) (Table 2).

Table 2: Histological grade for assessing cartilage damage severity.

Grade	Indication
0	Cartilage morphology is completely intact with no observable abnormalities.
1	The cartilage surface remains intact but shows changes in chondrocytes and minor alterations in morphology.
2	The presence of surface discontinuities indicates initial signs of cartilage degradation.
3	Development of vertical fissures extending into the cartilage layer.
4	Partial erosion of the cartilage surface, exposing underlying layers.
5	Complete denudation of the cartilage, leaving the subchondral bone exposed.
6	Significant deformation of the cartilage structure, indicating advanced degenerative changes.

2.8 STATISTICAL ANALYSIS

One - way analysis of variance (ANOVA) was performed to evaluate the microarchitecture of bone parameters in the rat and rabbit models, and a Tukey's HSD multiple comparison post hoc test was utilized to identify significant differences between the groups. The Kruskal-Wallis test and Dunn's multiple comparison tests were used to statistically compare the scores between groups for the non-parametric type of data, summarised in mean form. A p-value less than 0.05 was considered for a significant difference between groups. Micro-architecture bone parameters and histological evaluation statistical analysis were done using Graphpad Prism 7 (Graphpad Software, USA). Measurement consistency between different examiners was calculated using the intraclass correlation coefficient (ICC) using a two-way mixed effects model with absolute agreement. Intraclass correlation coefficient (ICC) analysis was performed using IBM SPSS Statistics 23 (SPSS Inc., USA), and an ICC > 0.7 is commonly used to indicate sufficient reliability.

3 RESULTS

3.1 GENERAL CONDITIONS OF ANIMAL MODELS

At the end of the 12-week study period, no significant differences in mortality or morbidity were observed between the control and OA-induced groups in either animal model. All animals remained clinically healthy, with no signs of pain or significant weight loss throughout the study. However, physical examinations revealed progressive joint effusion, swelling, and warmth in the affected knee joints of both species, with these symptoms being more pronounced in the rat model (Figure 1).

These clinical signs are consistent with the expected progression of OA and are likely attributable to disease development rather than procedural complications. Importantly, the study was conducted in accordance with ethical standards, and no undue harm or discomfort was inflicted on the animals. At the time of euthanasia, the average body weight of the rats was 497 g (range: 490–510 g), while the rabbits averaged 2.5 kg (range: 2.9–3.6 kg) (Figure 2), indicating stable health status throughout the experimental period.

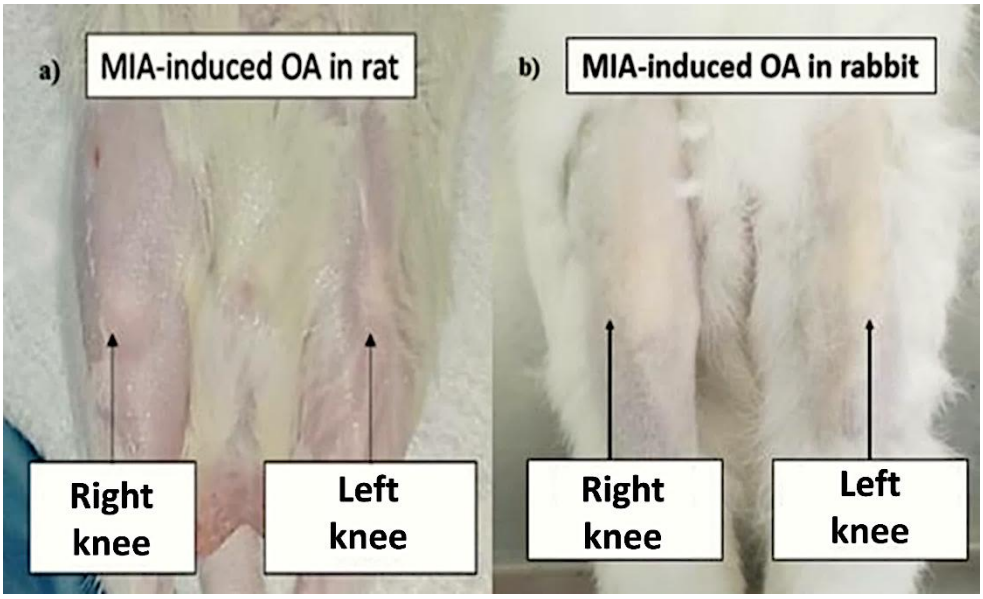


Figure 1. MIA-induced joint inflammation in rat and rabbit models. Photographs of the right knee joint at two weeks after MIA injection of rat (a) and rabbit (b) models.

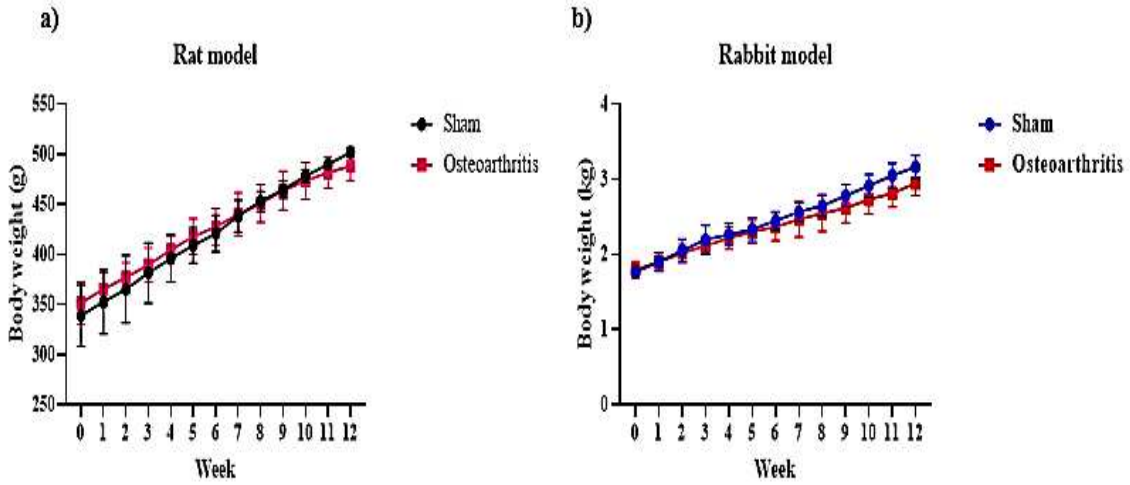


Figure 2. Time course of body weight changes in the rat (a) and rabbit (b) exposed to monosodium iodoacetate (MIA) until the end of the study (12 weeks). Data are presented as mean ± SD (n = 6).

3.2 MACROSCOPIC OBSERVATION OF FEMORAL AND TIBIAL PLATEAU

The study aimed to compare the pathological conditions of osteoarthritic joints in rat and rabbit models. The findings revealed that the rat model exhibited a significantly wider range of physiological conditions as compared to the rabbit model. After a 12-week study period, significant changes in the gross morphology of the femoral condyle and tibial plateau were noticed in both animal models. In a rabbit model, the sham femur and tibia exhibit smooth and intact surfaces, with no sign of erosion, fibrocartilage, or bone deformation. Both lateral and medial sides appear normal. In contrast, the osteoarthritic femur showed surface erosion and the presence of fibrocartilage on both lateral and medial sides. Similar to the femur, the OA tibia displayed erosion on both the lateral and medial sides. However, there are no signs of fibrocartilage formation.

In the rat model, the cartilage surfaces are smooth and show no signs of osteoarthritic changes, with both the lateral and medial sides appearing normal. In contrast, the rat's OA femur exhibits clear signs of bone deformation and the presence of fibrocartilage on both lateral and medial sides. Similarly, the rat's OA tibia also shows bone deformation and fibrocartilage on both sides.

Overall, both the rat and rabbit models demonstrate similar osteoarthritic changes, including surface erosion, presence of fibrosis, and bone deformation. However, the changes observed in the rat model are more severe compared to those in the rabbit model. Photographs of the femoral and tibial plateau's cartilage surface were taken and presented in Figure 3.

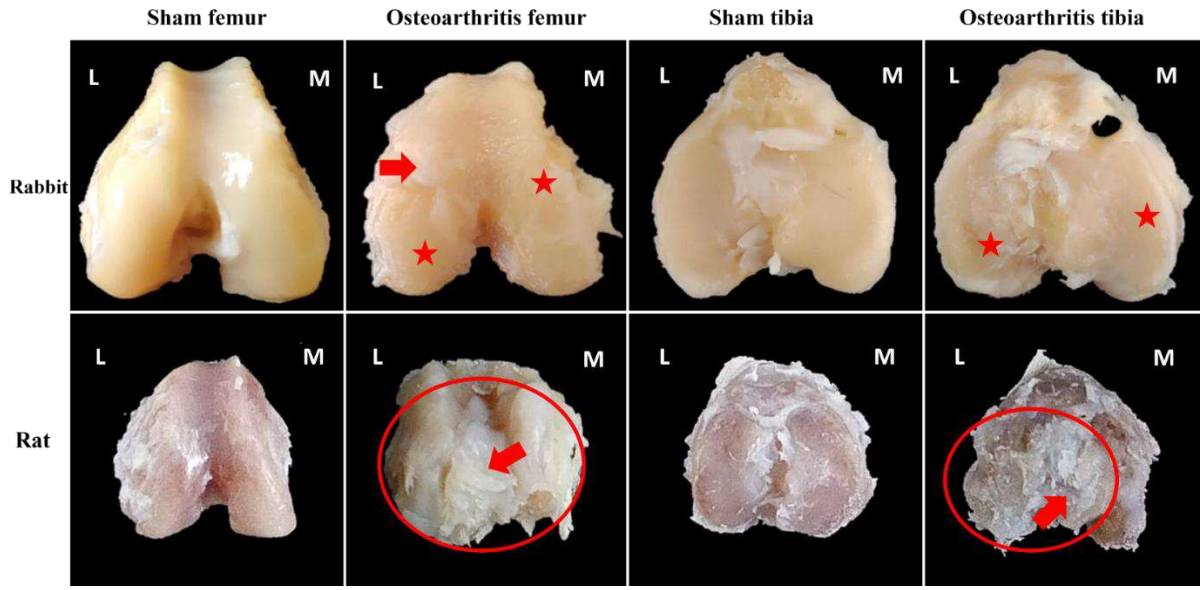


Figure 3. Gross morphology observation of rat and rabbit models' femoral condyle and tibial plateau. After a 12-week trial period, both groups showed osteoarthritic alterations characterized by surface erosion (star), the presence of fibrosis (arrow), and bone deformation (circle). L: Lateral, M: Medial.

3.3 MICRO-CT ASSESSMENT OF SUBCHONDRAL BONE

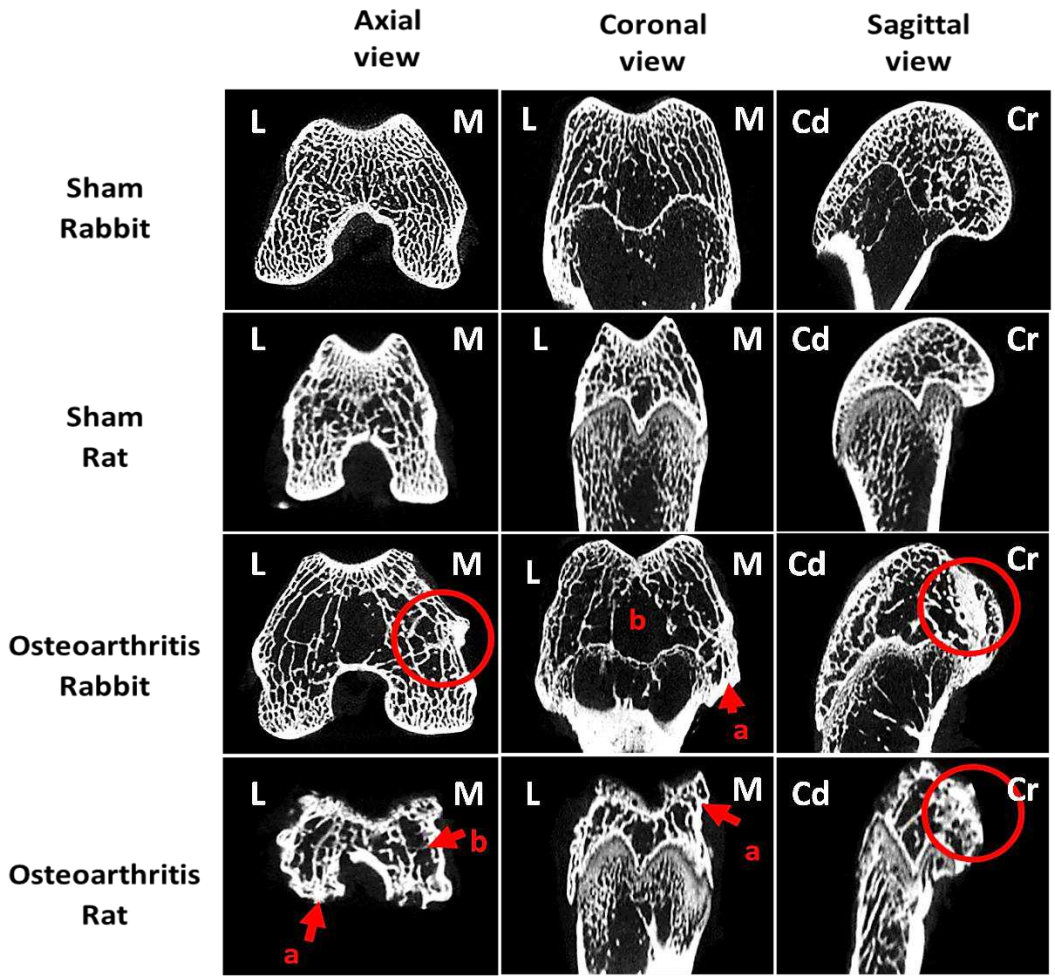


Figure 4. Two-dimensional micro-CT scans of axial, coronal, and sagittal views of the femur of the rat and rabbit models. Presence of sclerosis in both rat and rabbit OA models (red circle). Both rat rabbit OA models showed surface irregularities and osteophyte formation (a). Increased trabecular spacing and porosity were also observed in both rat and rabbit OA models (b). Cd: Caudal, Cr: Cranial, L: Lateral, M: Medial.

From Figure 4, the micro-CT scans were taken from axial, coronal, and sagittal views in 2D. In the sham groups for both rabbits and rats, the femurs appeared normal, without any of the osteoarthritic changes seen in the OA models. Specifically, no sclerosis was observed, and the bone surfaces remained smooth without irregularities or osteophyte formation. Additionally, the trabecular bone showed normal spacing and density.In the OA rabbit model, prominent sclerosis was noted, indicating abnormal hardening of bone tissue. This sclerosis was particularly evident on the medial side in both the axial and coronal views and on the cranial side in the sagittal view. There were distinct surface irregularities and osteophyte (bone spur) formation. These changes were observed on the medial side in the axial and coronal views and on the cranial side in the sagittal view, indicating new bone growth and uneven surfaces. The trabecular bone, which is the spongy part inside the femur, exhibited increased spacing and porosity, especially on the medial side in the axial and coronal views. The trabecular bone exhibited increased spacing and porosity.

In the OA rat group, sclerosis was prominently present on the medial side in the axial and coronal views and on the cranial side in the sagittal view. Surface irregularities and osteophyte formation were seen on the medial side in the axial and coronal views and on the cranial side in the sagittal view. Additionally, increased trabecular spacing and porosity were noted on the medial side in the axial and coronal views.

Overall, the rat model exhibits more severe OA changes compared to the rabbit model. In addition, the rat OA model displayed vivid bone deformation, which was not as pronounced in the rabbit OA model. This bone deformation was characterized by irregular and abnormal bone growth and shape.

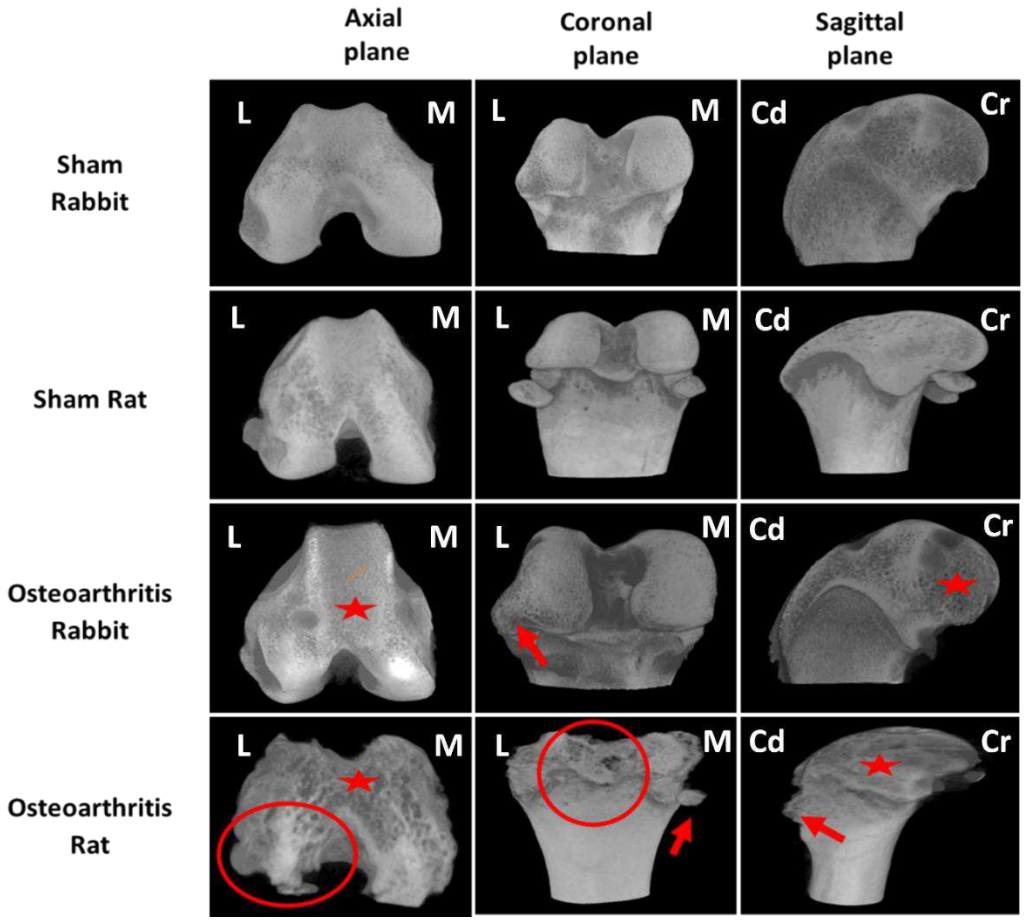


Figure 5. Three-dimensional micro-CT scans of axial, coronal, and sagittal views of the femur of the rat and rabbit models. Bone deformation (red circle), surface irregularities and osteophyte formation (red arrow), and erosion (star). Cd: Caudal, Cr: Cranial, L: Lateral, M: Medial.

From Figure 5, the micro-CT scans were taken from axial, coronal, and sagittal views in 3D. In the sham groups for both rabbit and rat models, the femur structures appeared normal with no abnormalities. Specifically, the axial, coronal, and sagittal views show no signs of bone deformation, surface irregularities, osteophyte formation, or erosion. The bone remains smooth, providing a baseline for healthy morphology.

In the OA rabbit model, erosion was evident on the lateral side in the axial view and on the cranial side in the sagittal view. Surface irregularities and osteophyte formation were observed on the lateral side in the coronal view, but bone deformation was absent in all views. In the OA rat model, intense bone deformation was observed on the lateral side in both the axial and coronal views. Erosion was present on the medial side in the axial view and on the cranial side in the sagittal view. Surface irregularities and osteophyte formation were noted on the medial side in the coronal view. Overall, the osteoarthritic changes in the rat model were more severe compared to the rabbit model.

3.4 QUANTITATIVE BONE MICRO-ARCHITECTURE ASSESSMENT

The micro-architecture of the femur bone was assessed using a set of five parameters namely bone volume to tissue volume (BV/TV) bone surface to volume ratio (BS/BV), trabecular thickness (Tb.Th), trabecular spacing (Tb.Sp), total porosity (PO). The result shows the micro-architecture parameters of the subchondral bone from the right stifle joints of the femur in both rat and rabbit models, comparing sham and OA conditions. In the rat model, the BV/TV ratio significantly increased in the OA group

(62.38 ± 6.13%), suggesting denser bone volume compared to the sham group (42.62 ± 1.18%). The BS/BV ratio also increases in the OA group (20.09 ± 4.62 mm^2/mm^3), indicating a more complex bone surface compared to the sham group (12.48 ± 1.55 mm^2/mm^3). Trabecular thickness (Tb.Th) decreases in the OA group (0.21 ± 0.02 mm) compared to the sham group (0.26 ± 0.03 mm), implying thinner bone structures. In comparison, trabecular spacing (Tb.Sp) significantly increases in the OA group (0.42 ± 0.07 mm) compared to the sham group (0.27 ± 0.02 mm), showing more separation between trabeculae. Total porosity (PO) also significantly increases in the OA group (70.70 ± 6.31%*) compared to the sham group (37.61 ± 6.13%), indicating higher bone fragility.

In the rabbit model, similar trends are observed. The BV/TV ratio significantly increased in the OA group (48.68 ± 1.53%) compared to the sham group (23.82 ± 1.09%). However, the BS/BV ratio remains relatively stable between the sham (13.46 ± 0.14 mm^2/mm^3) and OA groups (13.22 ± 0.61 mm^2/mm^3), suggesting less surface area change compared to rats. Tb.Th slightly but significantly increases in the OA group (0.23 ± 0.01 mm) compared to the sham group (0.20 ± 0.01 mm). Tb.Sp also shows a significant increase in the OA group (0.58 ± 0.04 mm) compared to the sham group (0.42 ± 0.01 mm). PO significantly increases in the OA group (68.26 ± 0.52%) compared to the sham group (53.83 ± 0.93%), but remains lower than that of the rats, indicating relatively less bone fragility.

Overall, while both models display significant osteoarthritic changes, the rat model shows more pronounced alterations in bone volume, trabecular spacing, and porosity, indicating a more severe impact of OA compared to the rabbit model. The results are documented in Table 3.

Table 3: Micro-architecture parameters of the subchondral bone of right stifle joints of femur obtained from rat and rabbit models at week 12.

	Mean±SD				
	BV/TV (%)	**BS/BV (mm^2/mm^3)**	**Tb.Th (mm)**	**Tb.Sp (mm)**	**PO (%)**
			Rat model		
Sham	42.62±1.18****	12.48±1.55	0.26±0.03	0.27±0.02***	37.61±6.13***
Osteoarthritis	62.38±6.13****	20.09±4.62	0.21±0.02	0.42±0.07***	70.70±6.31***
			Rabbit model		
Sham	23.82±1.09****	13.46±0.14	0.20±0.01	0.42±0.01***	53.83±0.93***
Osteoarthritis	48.68±1.53****	13.22±0.61	0.23±0.01	0.58±0.04***	68.26±0.52***

Results are presented as mean ± SD. BV/TV, bone to tissue volume ratio; BS/BV, bone surface to volume ratio; Tb.Th, trabecular thickness; Tb.Sp, trabecular spacing; PO, total porosity. Values with an asterisk (*) are significantly different ($p < 0.05$), * (0.0001), **** (<0.0001),**

3.5 HISTOPATHOLOGICAL GRADING AND STATISTICAL ANALYSIS

Table 4: Histological grade for rat and rabbit animal models (n=6).

Rat		Rabbit	
Sham	OA	Sham	OA
(median, range)	(median, range)	(median, range)	(median, range)
0	6	0	4.5
(0)	(5.0-6.0)	(0)	(4.0-5.0)

In Table 4, the histopathological grading of the femur's articular linings of the animal models is presented. The sham group of both animal models showed a grading of 0, indicating normal distribution of chondrocytes and smooth cartilage surfaces. This group had no evidence of cartilage damage. However, the rat OA group had a median grading of 6 (median range) at the end of the experiment. The articular cartilage in the rat OA group had surface discontinuity, which means that the surface of the cartilage was not smooth. Additionally, cartilage fibrillation was observed, which refers to the presence of small cracks on the surface of the cartilage. Furthermore, extensive cartilage erosion was observed, which means that the cartilage was wearing away and exposing the underlying bone. Finally, the exposed bone surface was observed, indicating that the cartilage was completely worn away in some areas.

In the rabbit OA model, the articular cartilage had a median of 4.5 (range 4.0–5.0) by the end of the study period. The grading showed that the articular cartilage changes were less severe in comparison to the rat OA model. The articular cartilage in the rabbit OA model showed some small cracks on the surface, but the changes were not as extensive as those observed in the rat OA model. The rat OA model exhibited more severe articular cartilage changes than the rabbit OA model, as per the observation. Although OA appeared milder in the rabbit model compared to the rat model, rabbits were chosen due to their anatomical and biomechanical similarities to the human knee, as well as their suitability for surgical procedures, advanced imaging, and histological analysis. These features make rabbits a valuable model for evaluating structural changes and potential therapeutic effects in a way that closely reflects human OA. These osteoarthritic changes observed in both animal models are illustrated in the histology images (Figure 6).

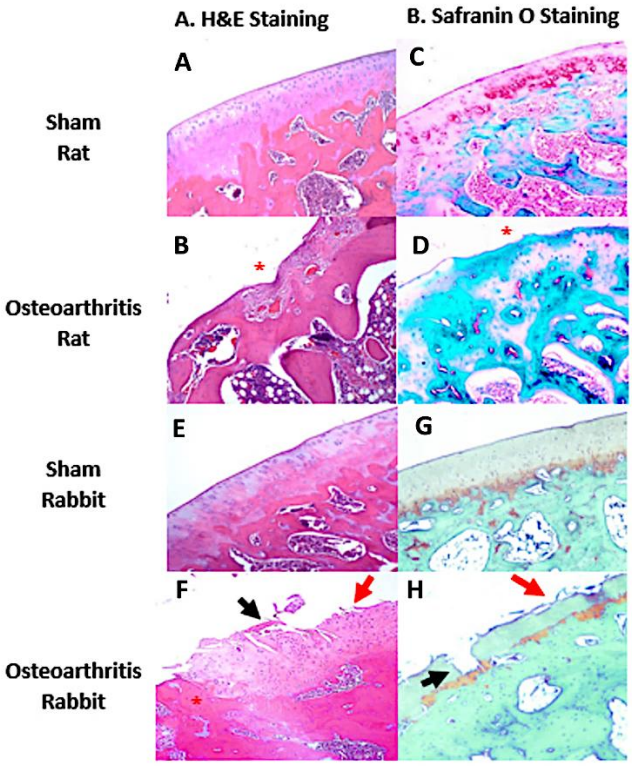


Figure 6. Representative histology images of femoral articular cartilage with H&E and Safranin O staining (200x magnification). A-D: rat model. E-H: rabbit model. Both OA groups showed cartilage fibrillation (red arrow) and extensive cartilage erosion (asterisk).

4 DISCUSSION

Animal models play a crucial role in osteoarthritis (OA) research, providing valuable insights into disease mechanisms and therapeutic responses. Rats and rabbits are among the most commonly used species due to their practicality, availability, and anatomical and physiological similarities to human joints (Kim & Cheon, 2012). Each model offers distinct advantages and limitations, and the choice between them should be guided by the specific objectives and design of the study.

Rats are relatively smaller than rabbits, which makes them convenient for housing and handling (Phipatanakul et al., 2012). They have smaller joints, which can be beneficial for certain experimental setups, particularly when considering imaging techniques. Moreover, their high metabolic rate might affect the progression of OA and response to interventions. Rats are also less expensive to maintain in laboratory settings (Little et al., 2010). On the other hand, rabbits are larger animals that provide more extensive joint surfaces for experimentation, which is advantageous for evaluating certain surgical procedures. However, rabbits have a slower metabolic rate than rats, which can impact the rate of disease progression and treatment responses. They may also increase the cost of maintenance and experimental procedures, and ethical considerations may be complex due to their larger sizes (Intema et al., 2010). Previous studies have reported that rabbits tend to develop milder MIA-induced OA compared to smaller rodents like mice or rats. This difference may be attributed to species-specific variations in joint anatomy, cartilage thickness, metabolism, and sensitivity to MIA dosage. For example, rabbits have thicker cartilage and a larger joint cavity, which may dilute the local concentration of MIA and reduce its cytotoxic effects (Janusz et al., 2002; Guzman et al., 2003).

During the 12 weeks of the study period, there was no significant difference in the mortality and morbidity in each animal model. Both animal groups showed no clinical signs of pain or reduction in body weight and were generally healthy. However, both groups showed joint effusion, swelling, and warmth, which gradually increased over time during physical observation. The effusion was more severe in the rats' OA joints compared to the rabbits' OA joints, which might be due to the active behaviour of the rats that constantly moved and socialised in the cage, while the rabbits were less active (Fabrcius et al., 2011). The rats were observed using their joints more than the rabbits, which might contribute to the burden of the mechanical loading. Mechanical loading difference was reported to affect OA development, and quadrupedal gait in mice has been shown to impact cartilage development intensely in the growth plate (Foster AD., 2019). However, despite the joint effusion and swelling, the animal's appetite and mobility were unaffected as their body weight continued to rise, and no signs of immobility were found. The rat's average body weight (range) was 497 g (490 - 510 g) during euthanasia. The rabbit's average body weight (range) was 2.5 kg (2.9 - 3.6 kg) during euthanasia. Harato & Yoshida (2015) reported that joint effusion does not necessarily cause immediate mobility issues. The body can adapt through various physiological mechanisms, enabling ongoing activity and weight maintenance (Harato & Yoshida, 2015).

From the macroscopic observation, significant cartilage loss was evident in osteoarthritic joints in the rat model compared to the rabbit model. This might be because the non-calcified cartilage layer in rats' joints is thinner than in the rabbit. Advanced imaging techniques, such as x-ray phase contrast imaging, have proven effective in visualizing and evaluating the thin cartilage layers in rat joints. However, these techniques highlight the thinness of rat cartilage, complicating the detection of early degenerative changes (Marenzana et al., 2012). Experimental models involving conditions like diabetes or OA exhibit significant alterations in cartilage composition and thickness, underscoring the delicate nature of rat cartilage (Atayde et al., 2012). In contrast, rabbit cartilage, which is thicker, has been effectively visualized using diffraction-enhanced imaging, enabling the detection of cartilage lesions within intact joints (Muehleman et al., 2013). The relatively thicker cartilage in rabbit models makes them preferable for studying joint diseases, as it provides a more substantial basis for observing degenerative changes and testing therapeutic interventions (Mantebea et al., 2022).

After 12 weeks of the study period, the gross morphology of the femoral condyle and tibial plateau showed significant changes in both animal models. In the beginning, there was smoothness with no surface irregularities observed on the articular cartilage of the joints from both animal models. On the lateral condyle cartilage of the femur, erosions were more noticeable but more evenly distributed on the articular cartilage of the tibia. At the end of the experiment, the rat OA model displayed more severe osteoarthritic features than the rabbit OA model. Osteophytes, or bone spurs, were observed in both animal models' femoral and tibial cartilage. Osteophytosis is regulated by several growth factors and cytokines, such as TGF-β secreted by chondrocytes, released following a joint tissue injury. This event might be caused by chondrocyte alteration after MIA administration, thus stimulating the formation of an aberrant bone via nestin-positive mesenchymal stem cells or osteoprogenitor cells (Takahashi et al., 2017). In the rat OA group, the medial condyle of the femoral and tibial cartilages showed more obvious degradation in joints, and bone deformation was achieved. This might be due to the rat's lifespan, which

is shorter than the rabbit's. The average lifespan of a rat is two years, while a rabbit is five years, which means the rat gets older faster than the rabbit. Our finding is consistent with a previous study that showed OA incidence and prevalence increase with age (Ro et al., 2020).

The 2D and 3D micro-CT morphological findings showed both rat and rabbit OA models revealed the presence of sclerosis. However, subchondral bone sclerosis was more severe in the rat OA model than in the rabbit OA model. Subchondral bone sclerosis, or thickening of bone, is considered an essential attribute of OA progression and is always associated with advanced late-stage OA. The subchondral bone acts as a shock absorber, distributes forces, and adapts to maintain joint conformation and prevent stress concentration (Burr and Gallant, 2012). Another study reported that OA might begin with subchondral bone adaptation by local stiffening to generate a steep stiffness gradient and induce high shear forces in the cartilage (Hu et al, 2021). Bone deformation also can be observed more vividly in the rat OA model. Bone deformation is one of the characteristics of late-stage OA. Since the rats' cartilage is thinner compared to the rabbit, it leads to rapid full-thickness cartilage loss in the rats (Poulsen et al., 2023). Additionally, osteophytes have been observed to develop in both animal models. Increased trabecular spacing and porosity were also observed in both rat and rabbit OA models. Same with 2D, 3D micro-CT images displayed extended OA severity in the rat OA model compared to the rabbit OA model. Even though some osteoarthritic alterations were seen in 2D and 3D images, micro-CT enables the morphological changes in bone to be precisely quantified. Therefore, several bone parameters were measured in this study.

The femur bone's micro-architecture was assessed using five parameters: BS/BV, Tb.Th, Tb.Sp, and PO. The results show the subchondral bone parameters from the right stifle joints of rat and rabbit models, comparing sham and OA conditions. In the rats model, the BV/TV ratio significantly increased in the OA group, suggesting denser bone compared to the sham group. The increase in BV/TV may represent an advanced OA, as late-stage OA is dominated by bone formation and higher osteoblastic activities (Yuan et al., 2014). The constant increase of BV/TV value may be due to more mechanical loading of the injected knee, as demonstrated in a previous study in which the injection of MIA into rats' knee joints triggered weight distribution changes in the hind paw, which resulted in bone loss (Foster AD., 2019). The BS/BV ratio also increased in the OA group, indicating a more complex bone surface compared to the sham group. Bone Marrow Lesions (BMLs) are a key feature of osteoarthritis, linked to increased bone volume fraction and trabecular thickness, resulting in a higher BS/BV ratio. These lesions involve sclerotic bone that is less well mineralized, which may weaken mechanical integrity and contribute to disease progression (Neogi, 2012). In OA, subchondral trabecular bone shows increased thickness and spacing, with a trend toward decreased trabecular number. These changes create a more plate-like structure, indicative of an increased BS/BV ratio (Muratovic., 2023). OA involves active bone remodelling, with heightened bone turnover and changes in mineralization, thought to be a response to altered mechanical loading. This remodelling contributes to the increased BS/BV ratio observed in osteoarthritic bones (Neogi, 2012). The increased BS/BV ratio, along with reduced mineral density in BMLs, may compromise subchondral bone, making it more susceptible to attrition and further joint damage (Neogi, 2012; Muratovic., 2023). Structural changes in subchondral bone, including an increased BS/BV ratio, are associated with pain and osteoarthritis progression, affecting the joint's biomechanical environment and leading to further cartilage loss and joint deterioration (Neogi, 2012). Understanding these changes in the BS/BV ratio and their role in osteoarthritis pathogenesis can help develop targeted therapies to modify bone remodelling processes and slow disease progression (Neogi, 2012).

Trabecular thickness (Tb.Th) decreased in the rat's OA group compared to the sham group, while trabecular spacing (Tb.Sp) significantly increased, showing greater separation between trabeculae. Osteoporotic conditions in rats show a significant reduction in trabecular thickness, which aligns with findings in OA models where trabecular thickness decreases compared to sham groups (Chen et al., 2019). Increased trabecular spacing is a hallmark of bone deterioration in conditions like osteoporosis and OA, attributed to the loss of trabecular connectivity and greater separation between trabeculae, as observed in ovariectomized rat models (Lee et al., 2019; Chen et al., 2019). The increase in trabecular spacing in OA can be linked to similar mechanisms of bone loss and structural degradation, leading to greater separation between trabeculae compared to healthy controls (Li et al., 2021). The ageing model also shows deteriorated trabecular microstructure, with reduced bone volume and increased spacing, similar to OA effects (Obara et al., 2022). Total porosity (PO) also significantly increased in the OA group compared to the sham group, indicating higher bone fragility. Research using a mouse model of OA has demonstrated that inducing OA results in significant increases in subchondral bone plate porosity, mainly due to heightened osteoclast activity, which thins the bone plate and creates perforations. These changes can be observed as early as two weeks post-induction, indicating that increased porosity is an early event in OA progression (Botter et al., 2011). In a rat model of post-traumatic OA, subchondral plate porosity was found to coincide with areas of mechanical load during movement, suggesting that mechanical stress contributes to the development of porosity, potentially exacerbating cartilage damage and OA progression (Iijima et al., 2016).

In rabbits, similar trends were observed. The BV/TV ratio significantly increased in the OA group compared to the sham group. However, BS/BV remained stable between sham and OA groups. Tb.Th slightly increased in the OA group compared to the sham group. Tb.Sp also increased significantly in the OA group compared to the sham group. PO significantly increased in the OA group compared to the sham group, but was lower than in rats. Overall, both models display significant osteoarthritic changes, with the rat model showing more pronounced alterations in bone volume, surface structure, and porosity, indicating a more severe OA impact compared to the rabbit model.

From the histopathological grading, the articular cartilage for the rat OA groups was graded with a median of 6 at the end of the experiment. Surface discontinuity indicated by cartilage fibrillation, extensive cartilage erosion, and the exposed bone surface was observed in both osteoarthritis-induced groups. For the rabbit OA model, the articular cartilage recorded a median of 4.5 (range 4.0–5.0) by the end of the study period. From the observation, the rat OA model displayed severe articular cartilage changes compared with the rabbit OA model. Too much mechanical loading generates gremlin-1, which in turn triggers NF-κB signalling. These events enhance the release of catabolic enzymes such as matrix metalloproteinase 13 (MMP13), disintegrin and metalloproteinase with thrombospondin motifs 5 (ADAMTS5) and subsequently cause articular cartilage degeneration (Chang et al., 2019).

Based on the findings of this study, the rabbit OA model may provide advantages for selected OA applications due to its anatomical similarity and translational relevance. One of the main reasons for this is that the degree of OA severity can be evaluated more accurately and precisely in the rabbit model. This is possible due to the ability to follow the progressive changes in articular cartilage and subchondral bone. The rabbit model is known to exhibit more similarities to human OA, particularly in terms of pathological changes in the joint. Rabbits' larger joint sizes make them ideal for surgical manipulations and therapeutic interventions. Their knee joints closely resemble human knees in cartilage thickness and biomechanics, making rabbits suitable for studying cartilage repair and degeneration (Zhang et al., 2023; Dilley et al., 2023). Notably, rabbit models have effectively shown the impact of human adipose-derived stem cells on cartilage healing, with significant cartilage repair and reduced joint effusion (Wang et al., 2024). Rats, being smaller and cost-effective, are practical for high-throughput studies. Their joint structures differ from humans, limiting the translatability of findings. However, rat models are invaluable for studying OA progression and pain, offering insights into joint degeneration and pain mechanisms (Hung et al., 2024; Williams et al., 2022; Fukui et al., 2023). Furthermore, the collection of synovial fluid for further studies is easier and more feasible in the rabbit model than in the rat model. This is because the rabbit's knee joint has a larger synovial cavity than the rat's knee joint. As a result, the amount of synovial fluid that can be collected is increased, making it more suitable for proteomic analysis and gene expression studies.

This study has several limitations, including the relatively small sample size and the absence of molecular analyses to further characterize OA progression. Additionally, the evaluation was performed at a specific time point, which may not fully reflect the temporal changes associated with disease development. Future studies with larger cohorts and longitudinal designs are warranted.

In summary, the rabbit OA model offers several advantages over the rat model for osteoarthritis research. It provides a more accurate evaluation of the degree of OA severity and better reflects the pathological changes observed in human OA. Additionally, it offers a more convenient method for collecting synovial fluid for further studies.

5 CONCLUSION

The rabbit osteoarthritis model demonstrates superior translational relevance compared to the rat model due to anatomical similarity to the human knee, slower disease progression, and improved feasibility for advanced imaging and synovial fluid analyses. This model is therefore recommended for future preclinical osteoarthritis studies.

6 DECLARATIONS

Ethics approval:

All animal procedures were approved by the Institutional Animal Care and Use Committee of Universiti Putra Malaysia (UPM/IACUC/AUP-R035/2021).

Consent To Participate:

Not applicable.

Consent To Publication:

Not applicable.

Data Availability:

The datasets generated and/or analysed during the current study are available from the corresponding author on reasonable request.

Competing interest:

The authors declare no competing interests.

Funding:

This work was supported by Universiti Putra Malaysia Research Management Centre IP Grant (GP/2020/9693000).

Authors' contribution:

All authors contributed to the study conception, design, data acquisition, analysis, and manuscript preparation. All authors read and approved the final manuscript.

7 ACKNOWLEDGEMENTS

All authors would like to thank the Faculty of Veterinary Medicine, Universiti Putra Malaysia, for the facilities and technical support provided throughout this study. Special thanks are also extended to our families and friends, Mohd Afiq Danial, Hawa Ebraham, Dr Nadwah Onwi, Pn Munirah Haris, Dr Nash, Dr Ammara, and Priscilla for their continuous encouragement and support.

8 REFERENCES

1. Artuzi FE, Brito RR, Scattone Silva R, Fernandes T, Lacerda S, Magalhães G, et al. Experimental models of osteoarthritis: A review. Acta Ortop Bras. 2016;24(6):330–333.
2. Atayde SA, de Araujo FA, Cunha V, Silva MJ, de Paula FJ. Influence of diabetes mellitus on the evolution of experimental osteoarthritis in rats. Diabetol Metab Syndr. 2012;4(1):40.
3. Botter SM, van Osch GJ, Waarsing JH, van der Linden JC, Verhaar JA, Pols HA, et al. Increased subchondral plate porosity in early OA mouse model. Arthritis Rheum. 2011;63(9):2690–2699.
4. Burr DB, Gallant MA. Bone remodelling in osteoarthritis. Nat Rev Rheumatol. 2012;8:665–673.
5. Calado GP, Lopes AJO, Junior LMC, Lima FDSCA, Silva LA, Pereira WS, et al. Chenopodium ambrosioides L. reduces synovial inflammation and pain in experimental osteoarthritis. PLoS One. 2015;10(11)\:e0141886.

6. Chang SH, Mori D, Kobayashi H, Mori Y, Nakamoto H, et al. Excessive mechanical loading promotes osteoarthritis through the gremlin-1–NF-κB pathway. Nat Commun. 2019;10:1–13.

7. Chen J, Wang D, Xiang Z, Li G. Subchondral bone deterioration in a rat model of osteoporosis and OA. J Orthop Surg Res. 2019;14(1):51.

8. Costa BM, Mariano LL, de Oliveira Menezes T, Silva Júnior VA. Alternatives for the treatment of osteoarthritis: review of the literature. Rev Bras Reumatol. 2017;57(1):105–110.

9. Dalevich M, Dyachenko A. Rat models of OA: reproducibility and standardization of behavioral outcomes. Curr Rheumatol Rev. 2024;20(1):13–25.

10. Dilley A, Bridges A, Thorp M. Rabbit knee joint biomechanics in OA modeling. J Biomech. 2023;151:111416.

11. Fabrcius AL, Bager Y, Peuhkuri K. Behavior and social interaction in laboratory rats: indicators of welfare and stress. Lab Anim. 2011;45(3):194–200.

12. Foster AD. The impact of bipedal mechanical loading history on longitudinal long bone growth. PLoS ONE. 2019;14\:e0211692.

13. Fukui N, Tanaka N, Okuno N. Gene expression analysis in synovial fluid of rat OA model. J Orthop Res. 2023;41(2):511–519.

14. Guzman RE, Evans MG, Bove S, Morenko B, Kilgore K. Mono-iodoacetate-induced experimental osteoarthritis. Osteoarthritis Cartilage. 2003;11(10):761–772.

15. Harato K, Yoshida H. Joint effusion and mobility: understanding the disconnect in osteoarthritis patients. J Orthop Sci. 2015;20(6):1057–1063.

16. Hu Y, Ding W, Ma Z, Wang Y, Song Y, et al. Mechanical adaptation of subchondral bone in OA: increased stiffness initiates cartilage degeneration. Bone Res. 2021;9(1):1–15.

17. Hung K, Wang Y, Lin C. Proteomic analysis of synovial fluid in rat OA model. Proteomics Clin Appl. 2024;18(1):2300058.

18. Iijima H, Aoyama T, Ito A. Mechanical stress-induced subchondral porosity in OA rat model. Osteoarthritis Cartilage. 2016;24(2):292–301.

19. Intema F, Hazewinkel HA, Gouwens D, et al. Comparison of osteoarthritis in rabbit and human knees. Arthritis Res Ther. 2010;12(5)\:R133.

20. Janusz MJ, Hookfin EB, Heitmeyer SA, Woessner JF Jr, Hsieh L, et al. Induction of osteoarthritis in the rat by surgical and chemical means. Osteoarthritis Cartilage. 2002;10(10):785–791.

21. Jones AC, Wilcox RK, Lee PD, Heeley DH, Ralph DJ, et al. High-resolution micro-CT imaging of trabecular bone structure. J Microsc. 2010;240(2):145–153.

22. Karhula SS, Finnilä MAJ, Piippo J, Tanska P, Joukainen A, Kauppinen S, et al. Quantitative evaluation of femoral head bone and cartilage structure in a mouse model of osteoarthritis using micro-CT and histology. J Orthop Res. 2018;36(3):643–653.

23. Kim SH, Cheon S. Comparative analysis of cartilage degeneration in OA models using various imaging techniques. Arthritis Res Ther. 2012;14\:R174.

24. Kloppenburg M, Berenbaum F. Osteoarthritis year in review 2019: epidemiology and therapy. Osteoarthritis Cartilage. 2020;28(3):242–248.

25. Kuyinu EL, Narayanan G, Nair LS, Laurencin CT. Animal models of osteoarthritis: classification, update, and measurement of outcomes. J Orthop Surg Res. 2016;11:19.

26. Lee K, Park J, Hwang J. Estrogen deficiency increases subchondral bone loss in ovariectomized rats. J Bone Miner Res. 2019;34(Suppl 1):126.

27. Lelovas KL, Xanthos TT, Thoma SE, Lyritis GP, Dontas IA. Useful animal models for the research of osteoarthritis. J Orthop Traumatol. 2014;15(4):263–271. doi:10.1007/s00590-013-1205-2.

28. Li X, Liu Z, Chen Y. Bone microarchitecture changes in OA and osteoporosis: similarities and distinctions. Bone Rep. 2021;14:100743.

29. Little CB, Smith MM. Animal models of osteoarthritis. Curr Rheumatol Rev. 2010;6(1):35–40.

30. Mantebea D, Zhu S, Chen Z. Emerging frontiers in rabbit osteoarthritis models: biomechanics and regenerative medicine. J Transl Med. 2022;20(1):567.

31. Marenzana M, Arhatari BD, Clarkin CE, Gouras P, Pitsillides AA, et al. X-ray phase contrast imaging reveals early osteoarthritis in mouse knee joint. Bone. 2012;50(4):972–978.

32. Muehleman C, Green DE, Tashman S. Visualization of articular cartilage lesions in intact joints using diffraction-enhanced imaging. Osteoarthritis Cartilage. 2013;21(9):1327–1332.

33. Muratovic D. Bone marrow lesions and BS/BV changes in human osteoarthritic subchondral bone. Bone. 2023;169:116616.

34. Musumeci G, Loreto C, Carnazza ML, Strehin I, Elisseeff JH. Biomaterials for articular cartilage repair: an overview of the progress in tissue engineering. Biomaterials. 2013;34(26):6143–6151.

35. Neogi T. The role of bone in osteoarthritis pathogenesis. Med Clin North Am. 2009;93(1):1–24.

36. Obara N, Hiraga Y, Iwasa T. Effects of age-related bone changes on OA progression. Aging Dis. 2022;13(3):776–786.

37. Palazzo C, Nguyen C, Lefevre-Colau MM, Rannou F, Poiraudeau S. Risk factors and burden of osteoarthritis. Ann Phys Rehabil Med. 2016;59(3):134–138.

38. Phipatanakul W, Ruffing MJ, Sullivan K, Huang S, Raby BA, Zeiger RS. Use of animal models in allergic disease research. J Allergy Clin Immunol. 2012;129(4):921–926.

39. Poulsen RC, Jain L, Dalbeth N. Re-thinking osteoarthritis pathogenesis: what can we learn (and what do we need to unlearn) from mouse models. Arthritis Res Ther. 2023;25(1):59.

40. Rutgers M, Saris DB, Dhert WJ, Creemers LB. Evaluation of histological scoring systems for tissue-engineered, repaired, and osteoarthritic cartilage. Osteoarthritis Cartilage. 2010;18(1):12–23.

41. Sulaiman SZ, Mokhtar A, Lau SF, Zakiah SZ. Subchondral bone and cartilage assessment using micro-CT and histology in osteoarthritis rabbit models. J Orthop Surg Res. 2022;17(1):140.

42. Sulaiman SZ, Tan WM, Radzi R, Shafie INF, Ajat M, Mansor R, et al. Comparison of bone and articular cartilage changes in osteoarthritis: a micro-computed tomography and histological study of surgically and chemically induced osteoarthritic rabbit models. J Orthop Surg Res. 2021;16:663.

43. Sulaiman SZS, Umran, NSS, Mohamed, S, Abu, J, Ng, AMH, Lau, BYC, Lai, KS, Ilias, N, Lau, SF, Ajat, M. Proteomic and morphologic analysis of bone and articular cartilage changes in osteoarthritic rabbits supplemented with Edible Bird's Nest (EBN). Malaysian Journal of Fundamental and Applied Sciences. 2024;20(6):1274-1287

44. Sun MM, Beier F. Chondrocyte hypertrophy in skeletal development, growth, and disease. Birth Defects Res C Embryo Today. 2012;100(4):352–366.

45. Takahashi I, Matsuzaki T, Hoso M. Long-term histopathological developments in knee-joint components in a rat model of osteoarthritis induced by monosodium iodoacetate. J Phys Ther Sci. 2017;29:590–596.

46. Trelle S, Reichenbach S, Wandel S, Hildebrand P, Tschannen B, Villiger PM, et al. Cardiovascular safety of non-steroidal anti-inflammatory drugs: network meta-analysis. BMJ. 2011;342\:c7086.

47. Van den Bosch MHJ. Osteoarthritis year in review 2020: biology. Osteoarthritis Cartilage. 2021;29(2):143–150.

48. Vinod N, Joghee N, Lakkakula R, Katiyar V. Anti-inflammatory activity of compounds isolated from Ficus glomerata Roxb. bark extract in experimental osteoarthritis. Biomed Pharmacother. 2018;107:1404–1413.

49. Wan Osman W, Abas F, Mokhtar A, Zakiah SZ. MIA-induced rat OA model and the effectiveness of natural compound therapy. BMC Complement Altern Med. 2017;17:280.

50. Wang Y, Ma W, Zhang L, et al. Adipose-derived stem cells promote cartilage repair in rabbit OA model. Stem Cell Res Ther. 2024;15(1):74.

51. Wang Y, Wei L, Zeng L, He D, Wei X. An overview of mouse models for osteoarthritis: comparison with human disease. Drug Des Devel Ther. 2018;12:455–464.

52. Williams FMK, Tamm A, Spector TD. Pain mechanisms in rodent OA models. Curr Rheumatol Rep. 2022;24(5):172–180.

53. Yuan XL, Meng HY, Wang YC, Peng J, Guo QY, Wang AY, et al. Bone-cartilage interface crosstalk in osteoarthritis: potential pathways and future strategies. Osteoarthritis Cartilage. 2014;22(8):1077–1089.

54. Zhang W, Chen J, Zhang Y, Sun W. Comparison of rabbit and rodent models in osteoarthritis research. Lab Anim Res. 2023;39:10.